Composites Part B 147 (2018) 12–21

Contents lists available at ScienceDirect

Composites Part B

journal homepage: www.elsevier.com/locate/compositesb

Morphological, rheological and electrical properties of composites filled with carbon nanotubes functionalized with 1-pyrenebutyric acid

L. Guadagno[a,*], M. Raimondo[a], L. Vertuccio[a], C. Naddeo[a], G. Barra[a], P. Longo[b], P. Lamberti[c], G. Spinelli[c], M.R. Nobile[a]

[a] Department of Industrial Engineering, University of Salerno, Via Giovanni Paolo II, 132, 84084, Fisciano, SA, Italy
[b] Department of Chemistry and Biology, University of Salerno, Via Giovanni Paolo II, 132, 84084, Fisciano, SA, Italy
[c] Department of Information and Electrical Engineering and Applied Mathematics, University of Salerno, Via Giovanni Paolo II, 132, 84084, Fisciano, SA, Italy

ARTICLE INFO

Keywords:
Nano-structures
Thermosetting resins
Electrical properties
Rheological properties
Functionalized carbon nanotubes
Non-covalent functionalization

ABSTRACT

Non-covalent functionalization of Multi Wall Carbon Nanotubes (MWCNTs) could provide a solution for preserving their electronic structure facilitating the nanocomposite process preparation. Functionalization of MWCNTs by π-stacking interaction between nanofiller and a pyrene derivative has been explored. The rheological properties of filled epoxy resins highlight very interesting benefits from this kind of functionalization. Besides its peculiar capability for preventing agglomeration in the nanofiller dispersion step, it also efficiently contributes to a decrease in the viscosity of the nanocomposites; hence contrasting one of the most relevant drawback related to the manufacturing processes of the nanocomposites at MWCNTs loading rates beyond the Electrical Percolation Threshold (EPT). Because no damage of MWCNTs occurs, sp^2 hybridization of carbon atoms is preserved together with the π-electron delocalization typical of polynuclear aromatic rings. Consequently, no deterioration in the electrical properties are detected; the measured EPT values are typical of nanocomposites containing embedded unfunctionalized MWCNTs (lower than 0.28 wt%), whereas for the electrical conductivity beyond the EPT, an enhancement is observed.

1. Introduction

Carbon nanotubes (CNTs) based composites represent a novel class of materials suitable for replacing many existing materials in several engineering fields due to their superior thermal, mechanical and electrical properties [1]. Furthermore, the dispersion of a small amount of CNTs in polymer composites improves the fracture interfacial rigidity and can stop micro-cracks evolution [2]. However, the development of such added-value polymer-based composites with specific functionalities and performance tailored to fulfill industrial requirements still presents several critical issues. In particular, carbon nanotubes dispersed in polymeric matrix usually tend to form aggregates, thus reducing reproducibility and performance in the expected properties. Another crucial parameter, which affects the efficiency of load transfer in such carbon-based polymer composites is the lack of a good interfacial adhesion between nanofiller and polymer [3,4]. Since the outer wall of pristine CNTs, as most of the other carbonaceous particles, is a chemically highly inert structure, one of the most promising solution to this drawback is certainly the application of methods for modifying the surface of nanoparticles. The chemical modifiers of particles have to be able to prevent agglomeration during dispersion processes, simultaneously preserving the electronic properties of the nanofillers and thus extending their potential applications. Hence, the degree of functionalization, as well as the nature of the functionalization, are key parameters to optimize the process of nanocomposite preparation in order to open the road towards real extended nanotechnology applications.

Therefore, a such topic is very actively discussed in current nanocomposite literature and several effective methods including covalent or non-covalent modification, biomolecule and metal ion binding, have been proposed to functionalize CNTs surfaces [5–8]. The covalent modifications, as well as the insertion of ionic groups on the surface of CNTs, produces hybridized sp^3 carbon, resulting in the loss of electrical conductivity of the nanofillers [9–11]. Instead, non-covalent modifications do not alter the electronic characteristics of the nanofiller. Song et al. proposed this last approach to disperse non-oxidized graphene flakes with non-covalent functionalization of 1-pyrenebutyric acid in nanocomposites able to manifest outstanding thermal conductivity (~1.53 W/mK) and improved mechanical properties (~1.03 GPa) [12]. Georgakilas et al. [13] have reported the study of non-covalent functionalization of graphene (G) and graphene oxide

* Corresponding author.
E-mail address: lguadagno@unisa.it (L. Guadagno).

https://doi.org/10.1016/j.compositesb.2018.04.036
Received 22 January 2018; Received in revised form 6 April 2018; Accepted 9 April 2018
Available online 10 April 2018
1359-8368/

(GO) for energy materials, biosensing, catalytic, and biomedical applications in a recent review. The review ends with a look at challenges and future prospects of non-covalently modified graphene and graphene oxide. The non-covalent functionalization involving mainly π–π interactions, van der Waals forces, hydrogen bonding, ionic interactions, or electron–donor acceptor complexes represents the strategic way to control the properties and improve the performance of G and GO in potential advanced applications [13]. In this paper, we report a non-covalent functionalization of Multi Wall Carbon Nanotubes (MWCNTs) by π–π stacking interactions with 1-pyrenebutyric acid in order to preserve the sp^2 hybridization of carbon atoms. The functionalized MWCNTs have been employed as filler in epoxy resins. The results highlight that 1-pyrenebutyric acid is useful to improve the dispersion without altering the electrical conductivity of the nanocomposites with respect to resins filled with unfunctionalized MWCNTs. The fluorescence analysis has highlighted strong interactions between the functional group 1-pyrenebutyric acid (1-PBA) and the surface of the employed nanotube. In fact, the interaction realized through interactions of type π–π stacking is capable to resist even after treatments of functionalized MWCNTs in boiling decaline as evidenced by the absence of 1-PBA in the remaining soluble fraction. The π–π interaction results in a significant preservation of electrical properties of the nanotubes, which favorable affect the electrical conductivity, and the value of electrical percolation threshold (EPT) of the formulated nanocomposites. In addition, the study of the rheological properties evidences a very relevant interest in this kind of functionalization. It is able to reduce the viscosity of the nanocomposites during the preparation steps of the nanocharged formulations. It is well known, in fact, that the increase in the viscosity of the nanocharged fluid formulations, due to the embedded nanofiller, represents one of the most limiting criticalities from an industrial point of view. The results here discussed highlight a very efficient lubricant effect of functionalized MWCNTs, which, depending on the nanofiller concentration, may result in a decrease in the viscosity even at values lower than that of the unfilled formulation.

2. Experimental section

2.1. Materials

2.1.1. Functionalization of multi wall carbon nanotubes with 1-pyrenebutyric acid

Multi wall carbon nanotubes, labeled in this work with the acronym CNT, have been produced via the Catalytic Carbon Vapor Deposition (CCVD) process and were obtained from Nanocyl S.A. CNTs which exit the reactor are then purified to greater than 95% carbon to produce the 3100 grade employed for this work. 1-Pyrenebutyric acid, labeled in the following with the acronym PY, was provided by Sigma-Aldrich.

The π– π stacking interaction between the PY and the unfunctionalized nanofiller CNT was obtained mixing in the reaction flask the 1-pyrenebutyric acid (≈0,100 g) and the nanofiller (≈1 g) in the CH_2Cl_2 dry (50 ml) (see Scheme 1). The blend was stirred for 2 h at room temperature. The product was filtered, washed with CH_2Cl_2 (30 ml) and dried overnight in vacuum. The product obtained, named CNT-PY, was ≈1.080 g.

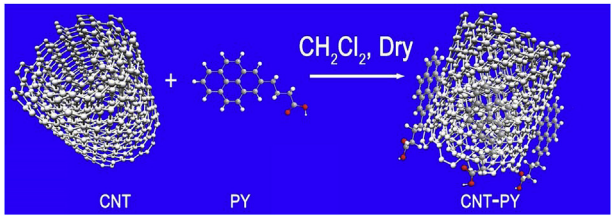

Scheme 1. Preparation of the functionalized carbon nanotubes CNT-PY.

2.2. Nanocomposite preparation

The functionalized carbon nanotubes CNT-PY were dispersed into the epoxy matrix to manufacture nanofilled composites. The epoxy matrix was prepared by mixing the epoxy precursor, tetraglycidylmethylenedianiline (TGMDA) (epoxy equivalent weight 117–133 g/eq), with the epoxy reactive monomer 1–4 butanedioldiglycidyl ether (BDE) that acts as a reactive diluent allowing to reduce the moisture content and to facilitate the dispersion step of nanofiller [14–21]. This mixture is labeled TB. The epoxy mixture TB was obtained by mixing TGMDA with BDE monomer at a concentration of 80%:20% (by wt) epoxide to flexibilizer. The curing agent 4,4′-diaminodiphenyl sulfone (DDS) was added at stoichiometric concentration with respect to all the epoxy rings (TGMDA and BDE), this mixture is named TBD in the following. Epoxy blend and DDS were mixed at 120 °C and the MWCNTs functionalized with 1-pyrenebutyric acid were added and incorporated into the matrix at loading concentrations of 0.05%, 0.1%, 0.32%, 0.5%, 0.64% and 1% by weight by using a ultrasonication for 20 min (Hielscher model UP200S-24 KHz high power ultrasonic probe). All the mixtures were cured by two-stage curing cycles: a first isothermal stage is carried out at the lower temperature of 125 °C for 1 h and then a second isothermal stage at higher temperatures up to 200 °C for 3 h.

2.3. Methods

High-Resolution Transmission Electron Microscopy (HRTEM) characterization was performed on a Jeol 2010 $LaBa_6$ microscope operating at 200 kV. MWCNTs were dispersed (in ethanol) by ultrasonic waves for 30 min. The obtained suspension was dropped on a copper grid (holey carbon).

Raman spectra were collected at room temperature with a Micro Raman spectrometer Renishaw inVia operating with a 514 nm laser source.

Infrared spectra were obtained in absorbance by using a FTIR-Bruker Vertex 70 spectrophotometer with a resolution of 4 cm^{-1} (32 scans collected).

Field Emission Scanning Electron Microscope (FESEM) images of the epoxy composites filled with functionalized CNTs were obtained using SEM (mod. LEO 1525, Carl Zeiss SMT AG, Oberkochen, Germany). All the samples were placed on a carbon tab previously stuck to an aluminum stub (Agar Scientific, Stansted, UK) and were covered with a 250 Å-thick gold film using a sputter coater (Agar mod. 108 A). Nanofilled sample sections were cut from solid samples by a sledge microtome. These slices were etched before the observation by SEM. The etching reagent was prepared according to a previous reported procedure [14,17,20,21].

Fluorescence spectra were recorded by a Varian Cary Eclipse spectrophotometer using chloroform as solvent.

Thermogravimetric analysis (TGA) was carried out in air using a Mettler TGA/SDTA 851 thermal analyzer. The temperature range was 25–1000 °C at a heating rate of 10 °C min^{-1}. The weight loss was recorded as a function of the temperature.

Rheological oscillatory tests, on uncured samples in the liquid state, were carried out using a Physica MCR 301 (Anton Paar) rotational rheometer equipped with a parallel plate geometry (50 mm diameter, 1 mm gap). The ternary TGMDA-BDE-DDS mixture (named TBD in the following), two dispersions of the multiwalled carbon nanotubes 3100 (Nanocyl) in the TBD matrix (named TBD + 0.1%CNT and TBD + 0.25%CNT) and two dispersions of the functionalized MWCNTs with 1-pyrenebutyric acid (named TBD + 0.09%CNT-PY and TBD + 0.225%CNT-PY) were analyzed. In the case of the dispersions of the CNT-PY in the TBD matrix, the contribution of the functional groups has been subtracted, then the weight concentrations refer exclusively to the multiwalled carbon nanotubes.

Strain sweep tests, at the frequency of 1 rad/s, were performed in

order to determine the linear viscoelastic region. Frequency sweep test at 50 °C and 75 °C were performed, within the linear viscoelasticity region, varying the angular frequency from 10^{-2} to 10^{2} rad/s.

The electrical characterization of the nanocomposites was performed on disk shaped specimens of about 2 mm of thickness and 50 mm of diameter. In order to reduce possible surface roughness and to ensure an ohmic contact with the measuring electrodes, the samples were coated by using a silver paint with a thickness of about 50 μm and a surface resistivity of 0.001 Ω·cm. The measurement system, remotely controlled by the software LABVIEW®, is composed by a suitable shielded cell with temperature control, a multimeter Keithley 6517A with function of voltage generator (max ± 1000 V) and voltmeter (max ± 200 V) and an ammeter HP34401A (min current 0.1 μA) for samples above the EPT. For those below the percolation threshold the system is composed only by a multimeter Keithley 6517A with function of voltage generator (max ± 1000 V) and pico-ammeter (min current 0.1 fA).

3. Results and discussion

3.1. Characterization of pristine (CNT) and functionalized multi wall carbon nanotubes (CNT-PY)

3.1.1. Morphological and spectroscopic analysis of pristine multi wall carbon nanotubes (CNT)

HRTEM images of CNT are shown in Fig. 1.

HRTEM analysis provides the geometrical parameters shown in Table 1.

Raman and FTIR spectra collected for pristine CNT nanofiller are shown in Fig. 2. Raman spectrum (see Fig. 2a) exhibits two strong bands, the D mode (1350 cm^{-1}) and the tangential stretching G mode (1586 cm^{-1}) in the investigated spectral range. The D-band at ~1350 cm^{-1} is identified with defects present in the carbon aromatic structure.

The D-band is a double-resonance Raman mode affected by defects in the graphene structure of the wall. This band can be used for material characterization to probe and monitor structural modifications of the nanotube sidewalls that come from the introduction of defects and the attachment of different functional groups. The G-band consists of two components that are generally distinguishable in the spectrum of single wall carbon nanotubes with a peak at 1590 cm^{-1} (G^{+}) and another at about 1570 cm^{-1} (G^{-}). The G^{+} feature is associated with carbon atom vibrations along the nanotube axis (LO phonon mode). The G^{-} feature, in contrast, is associated with vibrations of carbon atoms along the circumferential direction of the SWCNTs. In our spectrum, we observe a single peak for the G-band because the G^{+} - G^{-} splitting in MWCNTs is both small in intensity and smeared out by the effect of the diameter distribution within the individual MWCNTs, and the ensemble of MWCNTs. The G-band feature only exhibits a weakly asymmetric characteristic lineshape, with a peak appearing close to the graphite frequency (1582 cm^{-1}).

Table 1
Details of CNT.

Subject	Parameter	Value
CNT	Length (m)	$100 \times 10^{-9} \div 1 \times 10^{-6}$
	Diameter (nm)	9÷19
	Number of walls (/)	4÷11
	Walls separation (nm)	[0.35]

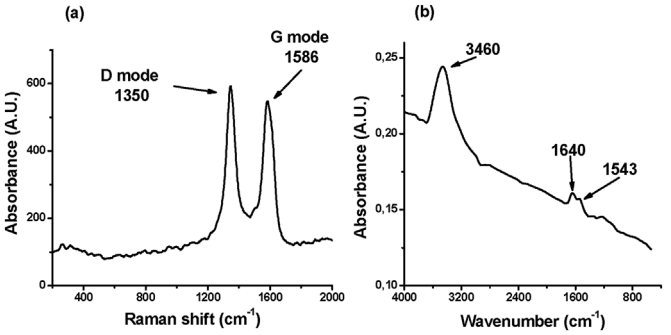

Fig. 2. Raman spectrum (a) and FTIR spectrum (b) of pristine CNT.

The intensity and characteristics of this band give information on the order of graphitic layers in the carbon nanostructured forms. In particular, a high ratio R of intensities of the D and G bands ($R = I_D/I_G$) indicates a high quantity of structural defects. The R-value of our MWCNTs is 1.19.

This small value highlights that an amount of defects (and therefore chemical species or functional groups are attached to the walls of MWCNTs) are always present also on MWCNTs which are commercialized as unfunctionalized nanoparticles. To obtain information on the nature of the functional groups attached to the wall of MWCNTs, the sample has been analyzed by FTIR investigation.

FTIR studies have been performed in the range 400–4000 cm^{-1} for the identification of the functional groups attached on the surface of the MWCNTs. FTIR spectroscopy has been used extensively in the structural determination of functional groups bonded to carbon based nanofillers. Fig. 2b shows the FTIR spectrum of the pristine CNT.

As observed in the spectrum, together with expected signals (i.e. C-C stretch at 1640 cm^{-1} and 1543 cm^{-1}, due to skeletal vibrations from unoxidized domains) other peaks are present. In particular, the spectrum shows the presence of oxygenated functional groups (mainly hydroxyl and epoxide), whose concentration is not negligible. The presence of different type of oxygen functionalities was confirmed by the bands at 3460 cm^{-1} (O-H stretching vibrations), at 1220 cm^{-1} (C-OH

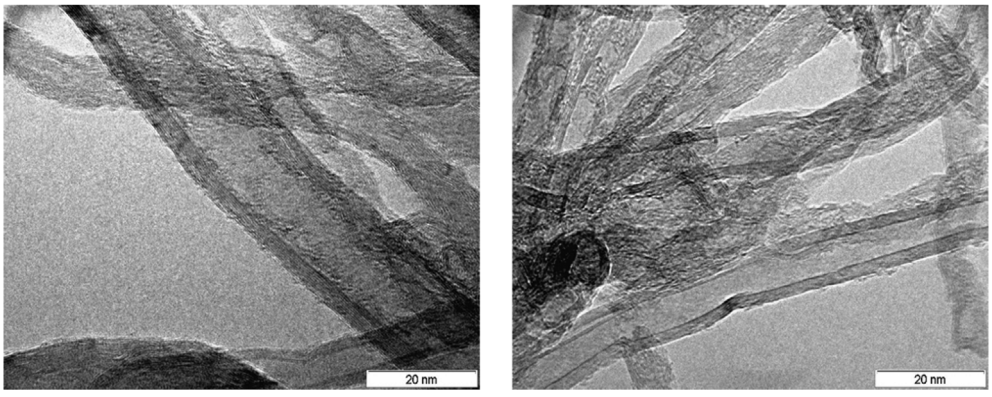

Fig. 1. High resolution transmission electron microscope (HRTEM) images of pristine CNT.

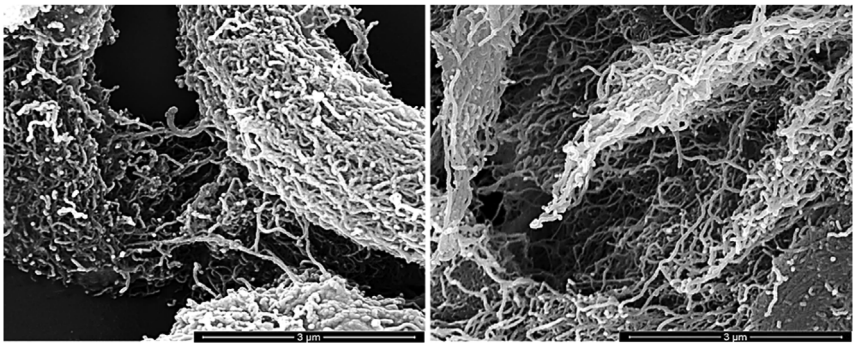

Fig. 3. FESEM images of unfunctionalized CNT (on the left side) and functionalized CNT-PY (on the right side).

stretching vibrations), and at 1024 cm^{-1} (C-O stretching vibrations). It is worth noting that the value of the O-H stretching vibrations and the profile of this band is typical of non-hydrogen-bonded or "free" hydroxyl group in the solid phase. This last observation highlights that the -OH groups are in small amount and spaced. This spatial position is able to hinder intermolecular hydrogen bonding between carbon nanotubes. This can strongly contribute to have a better distribution with negligible aggregates in the polymeric matrix as shown in the next paragraph.

3.1.2. Morphological and spectroscopic analysis: comparison between functionalized (CNT-PY) and unfunctionalized carbon nanotubes (CNT)

FESEM images of unfunctionalized CNTs (on the left side) and functionalized CNT-PY (on the right side) are shown at the same magnification in Fig. 3.

HRTEM images of unfunctionalized CNT (on the left side) and functionalized CNT-PY (on the right side) are shown in Fig. 4.

The comparison between functionalized CNT-PY and unfunctionalized CNT performed both by FESEM and HRTEM highlights a better separation of the functionalized CNT-PY with respect to the unfunctionalized CNT.

3.1.3. Fluorescence and FTIR spectra

Fluorescence spectrum of 1-pyrenebutyric acid in chloroform measured under an excitation wavelength of 298 nm at room temperature is shown in Fig. 5 (see black spectrum a), where, for comparison, the fluorescence spectrum the soluble fraction in boiling decaline is also shown (see blue spectrum b). The spectrum of 1-pyrenebutyric acid shows the typical band at the maximum wavelength of 475 nm which disappears in the blue spectrum b corresponding to the fraction extracted by boiling decaline. This is a clear evidence of the strong interaction between MWCNTs and the 1-pyrenebutyric acid. In fact, the extraction with boiling decaline does not contain pyrene in the soluble fraction.

The strong interaction between pyrene and CNTs has already reported by other authors. Zhang et al. through spectroscopic evidence and molecular simulation investigation evidenced the stronger π–π stacking interaction between the nanotubes and pyrene molecules over

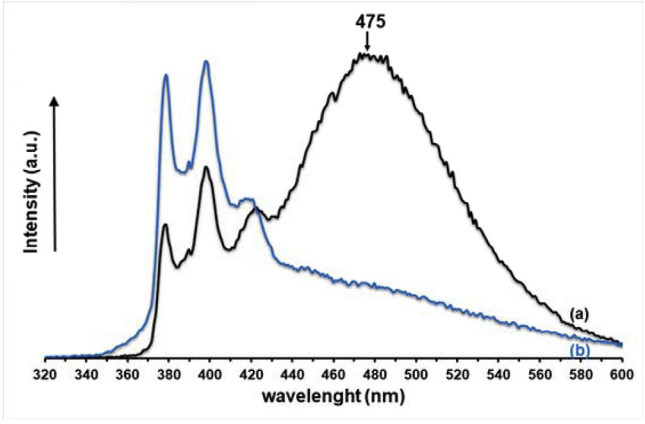

Fig. 5. Fluorescence spectra of 1-pyrenebutyric acid (see black spectrum a) and the soluble fraction in boiling decaline (see blue spectrum b). (For interpretation of the references to colour in this figure legend, the reader is referred to the Web version of this article.)

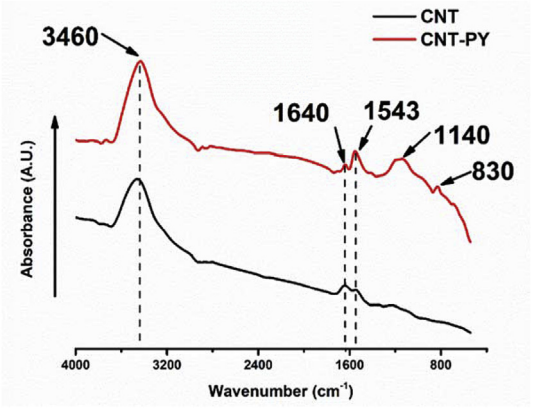

Fig. 6. FTIR spectra of the functionalized CNT-PY and unfunctionalized CNT.

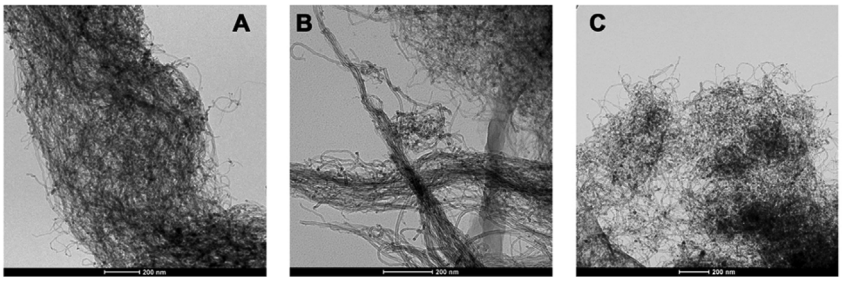

Fig. 4. HRTEM images of unfunctionalized CNT (A) and functionalized CNT-PY (B and C).

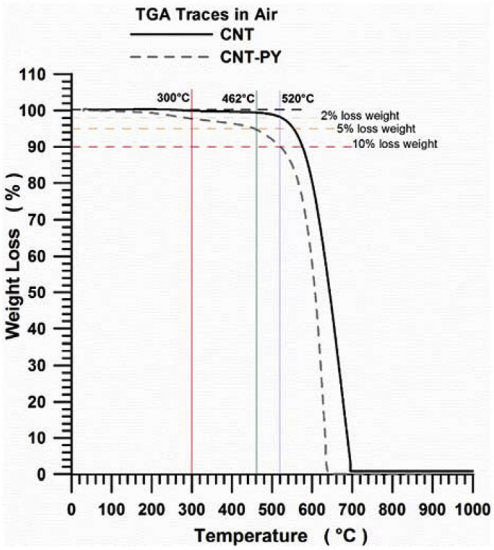

Fig. 7. Thermogravimetric curves of CNT and CNT-PY.

pyrene dimers, which leads to the formation of pyrene-carbon nanotube complexes [22].

FTIR spectrum of the functionalized CNT-PY is shown in Fig. 6, which also shows the spectrum of the unfunctionalized sample CNT for comparison.

The spectrum of the functionalized CNT-PY shows the bands assigned to C-C stretching vibrations of pyrene butyric acid in the broad region of 1200-800 cm^{-1}. The wideness of this band is due to the overlapping of C-C stretching vibrations with signals due to bending vibrations of CH_2 groups (ω CH_2 and τ CH_2). Furthermore, the C-C ring stretch signals between 1600 and 1460 cm^{-1} seem to be more intense than those of the unfunctionalized CNT and very week signals appear in the range between 3100 and 3000 cm^{-1} corresponding to C-H aromatic stretching. These results confirm the success of the performed functionalization.

3.1.4. Thermogravimetric characterization

Thermogravimetric curves in air for pristine CNT and functionalized CNT-PY are shown in Fig. 7. It is worth to note that pristine CNT nanotubes are stable up to about 520 °C and at this temperature the functionalized CNT-PY show a weight loss of approximately 10 wt%. This weight loss, exactly corresponding to the amount of functional groups attached to carbon nanotubes, quantified at 10 wt%, is attributable to the degradation of the pyrene moieties.

3.2. Characterization of epoxy composites

3.2.1. Rheological properties

The complex viscosity values for the liquid dispersions containing the unfunctionalized (CNT) and the functionalized (CNT-PY) multi wall carbon nanotubes in the TBD uncured matrix are shown in Figs. 8 and 9, at the temperatures of 50 and 75 °C respectively. In the following, the slight difference that is reported for the carbon nanotube concentration between the TBD-CNT and the TBD-CNT-PY dispersions is related to the fact that the contribution of the functional groups has been subtracted in the dispersions including the CNT-PY nanotubes, as mentioned in the experimental section.

The rheological results evidence that both the TBD + 0.1%CNT and the TBD + 0.09%CNT-PY dispersions are characterized by a Newtonian behavior in the whole frequency range analyzed; the inclusion of a low content of carbon nanotubes does not modify, in fact, the Newtonian behavior of the pure TBD epoxy matrix (Figs. 8a and 9a). However, it is of considerable interest to observe that, if on one hand, the addition of 0.1 wt% of unfunctionalized multi wall carbon nanotubes in the TBD matrix determines a significant increase in the viscosity of the TBD epoxy uncured matrix (as usual observed in CNT nanocomposites [16,23–33]), on the other hand, the inclusion of 0.09 wt% CNT-PY functionalized carbon nanotubes decreases the complex viscosity of the TBD uncured matrix.

As the CNT loading increases, the Newtonian plateau is not observed at low frequencies for both the TBD + 0.25%CNT and the TBD + 0.225%CNT-PY dispersions, as shown in Figs. 8b and 9b at the temperatures of 50 and 75 °C respectively. Indeed, a shear thinning behaviour in complex viscosity is detectable at the temperature of 50 °C (Fig. 8b) and it becomes even more significant at the temperature of 75 °C (Fig. 9b). The presence of a shear thinning in the complex viscosity of the uncured dispersions can be attributed to the formation of an interconnected network in the nanocomposite [16,23–33]. The critical CNT concentration required to obtain the network is generally labelled the rheological percolation threshold. The rheological results clearly indicate that both the TBD + 0.25%CNT and the TBD + 0.225%CNT-PY dispersions are above the percolation threshold, with the percolation rheological threshold decreasing with increasing the temperature, in agreement with literature results [25,27,29,31,33].

In particular, the inclusion of 0.25 wt% of the unfunctionalized CNT in the TBD determines a strong increase in the viscosity of the TBD epoxy matrix both at T = 50 and 75 °C so that, at low frequencies, the η* values of the TBD + 0.25%CNT dispersion are about two orders of magnitude greater than the corresponding viscosity values of the pure TBD liquid matrix. Conversely, when the functionalized nanotubes CNT-PY are added to the TBD matrix, the TBD + 0.225%CNT-PY dispersion shows viscosity values similar (at lower frequencies) or even lower (at higher frequencies) than the viscosity of the TBD epoxy matrix at the temperature of 50 °C (Fig. 8b). Finally, at T = 75 °C and lower frequencies, a significant decrease of the viscosity of the TBD + 0.25%CNT dispersion is obtained with the use of the functionalized CNT-PY nanotubes (Fig. 9b) in the TBD matrix.

The storage modulus values, G′, measured at the temperature of 75 °C for both the TBD + 0.25%CNT and the TBD + 0.225%CNT-PY dispersions are reported in Fig. 10a.

In literature, it has been reported that the inclusion of the nanofillers gradually modifies the terminal liquid-like behavior of the pure matrix (i.e. G′ scaling about as ω^2) so that the transition from liquid-like to solid-like behaviour, due to the formation of an interconnected network in the nanocomposite, can occur in the case of thermoplastic [23–27,29,32,33] matrices as well as in case of epoxy and polyester matrices [16,28,30,31].

In Fig. 10a the storage modulus results at T = 75 °C show that the inclusion of 0.25 wt% CNT in the TBD epoxy matrix produces a plateau in G′ at low frequencies indicative of a clear solid-like behaviour. The TBD + 0.25%CNT liquid dispersion is, therefore, well above the percolation threshold. In the case of the TBD + 0.225%CNT-PY dispersion, the dependence of G′ on the frequency weakens, scaling about as $\omega^{0.5}$, suggesting that also this sample is above the percolation threshold.

The rheological percolation threshold can be observed more clearly in the van Gurp-Palmen plot [34] where the phase angle (δ) is plotted versus the absolute value of the complex modulus, |G*|, as suggested in literature [25,33,35]. In Fig. 10b the van Gurp-Palmen plots for the TBD Newtonian uncured matrix as well as for the TBD + 0.25%CNT and the TBD + 0.225%CNT-PY dispersions are reported. At low complex moduli, the TBD matrix shows the flow behaviour of a viscous fluid since the curve approaches a phase angle of 90°; conversely a significant decrease of the phase angle at low complex moduli can be detected in the case of the two CNT dispersions. Indeed, both the dispersions clearly resemble the behaviour of an elastic solid, whose corresponding equilibrium modulus can be determined extrapolating the curves to a phase angle of 0°. The van Gurp-Palmen plot, then, confirms that both the TBD + 0.25%CNT and the TBD + 0.225%CNT-PY dispersions are above the rheological percolation threshold.

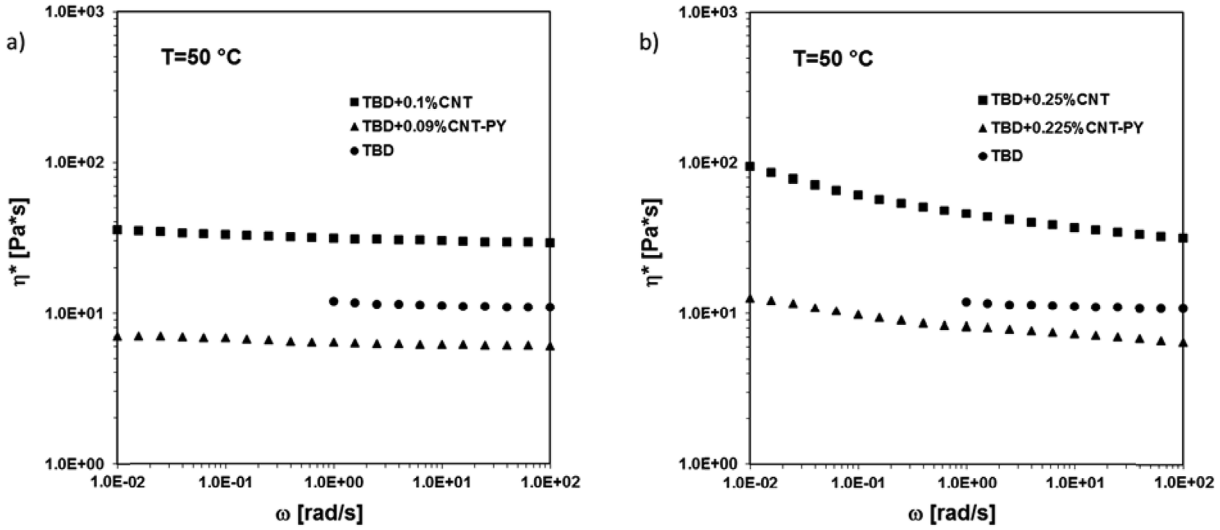

Fig. 8. Complex viscosity (η*) vs frequency (ω) at T = 50 °C for: a) the TBD epoxy matrix, the TBD + 0.1%CNT and the TBD + 0.09%CNT-PY liquid dispersions; b) the TBD epoxy matrix, the TBD + 0.25%CNT and the TBD + 0.225%CNT-PY liquid dispersions.

Summarizing, the rheological study has shown that the complex viscosity of the nanocomposite at 0.09 wt% loading of the CNT-PY nanotubes falls below that of the neat uncured TBD epoxy matrix. In literature, a decrease in the viscosity of the matrix has been reported for low contents of multi-walled carbon nanotubes in polystyrene [36] and nylon [37]. It can be assumed that the CNT-PY nanotubes act as a plasticizer at the low concentrations, so that the particle-particle interaction was not established within the matrix. Increasing the carbon nanotube content above the rheological percolation threshold, the viscosity of the CNT-PY dispersion increases above that of the neat TBD matrix. However, thanks to the use of the functionalized CNT-PY nanotubes, the increase in viscosity of the dispersion including the amount of 0.225w% CNT-PY was very moderate, thus allowing to limit one of the major drawbacks of the use of carbon nanotubes in the processing of epoxy nanocomposites.

3.2.2. Morphological investigation of the carbon-based epoxy nanocomposites

A special attention is paid in literature to the preparation of nanocomposites with non-aggregated nanoparticles because dispersion of nanofillers is a key problem in nanotechnology industrialization [38]. In this paper, the dispersion of unfunctionalized and functionalized CNTs in the polymeric matrix was analysed by SEM investigation on etched samples. Fig. 11a–b show SEM images of the fracture surface of the epoxy-based composites filled with 1 wt% loading of CNT and CNT-PY in two different zones. The etching procedure allows a clear observation of the nanofiller distribution. The functionalized carbon nanotubes (CNT-PY) appear well dispersed in the polymeric matrix, although the amount of MWCNTs is quite high (1 wt% of CNT-PY).

Unfunctionalized CNTs tend to form bundles, or networks of nanotubes more easily with respect to CNT-PY.

A very interesting aspect highlighted by the comparison in morphological features of these two kinds of nanocomposites is related to the interaction between nanotubes and matrix. The morphological analysis shows that, although the etching procedure was exactly the same for both typologies of samples, unfunctionalized CNTs clearly appear to be less bound to the resin matrix. A comparison between the SEM images of the two different nanocomposites (fig. 11a and b)

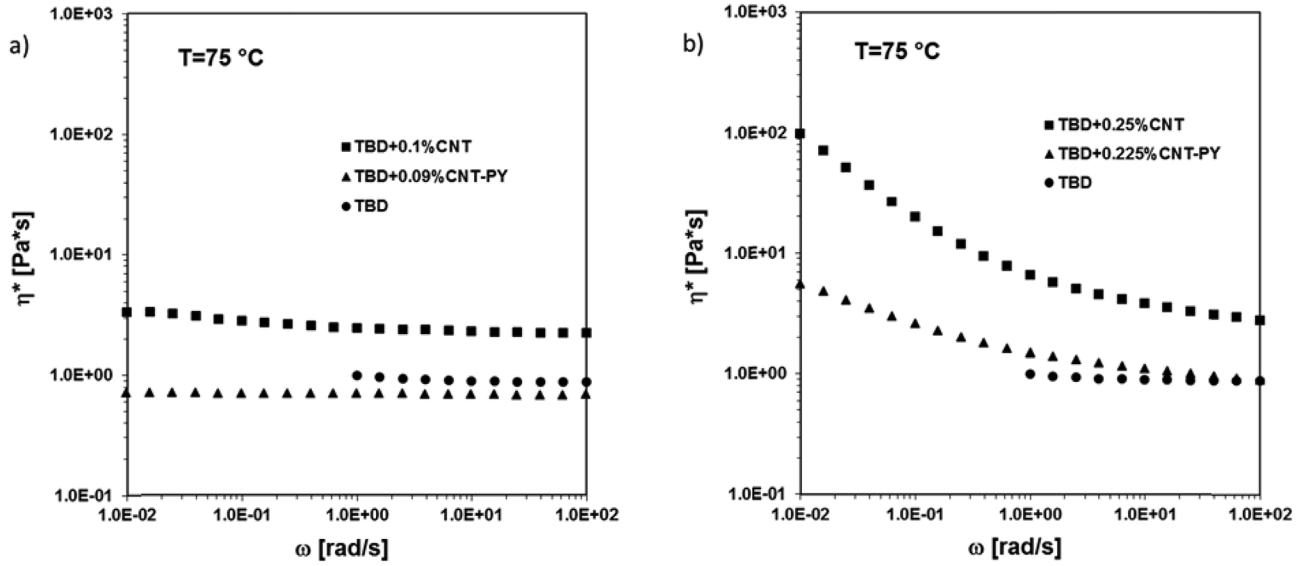

Fig. 9. Complex viscosity (η*) vs frequency (ω) at T = 75 °C for: a) the TBD epoxy matrix, the TBD + 0.1%CNT and the TBD + 0.09%CNT-PY liquid dispersions; b) the TBD epoxy matrix, the TBD + 0.25%CNT and the TBD + 0.225%CNT-PY liquid dispersions.

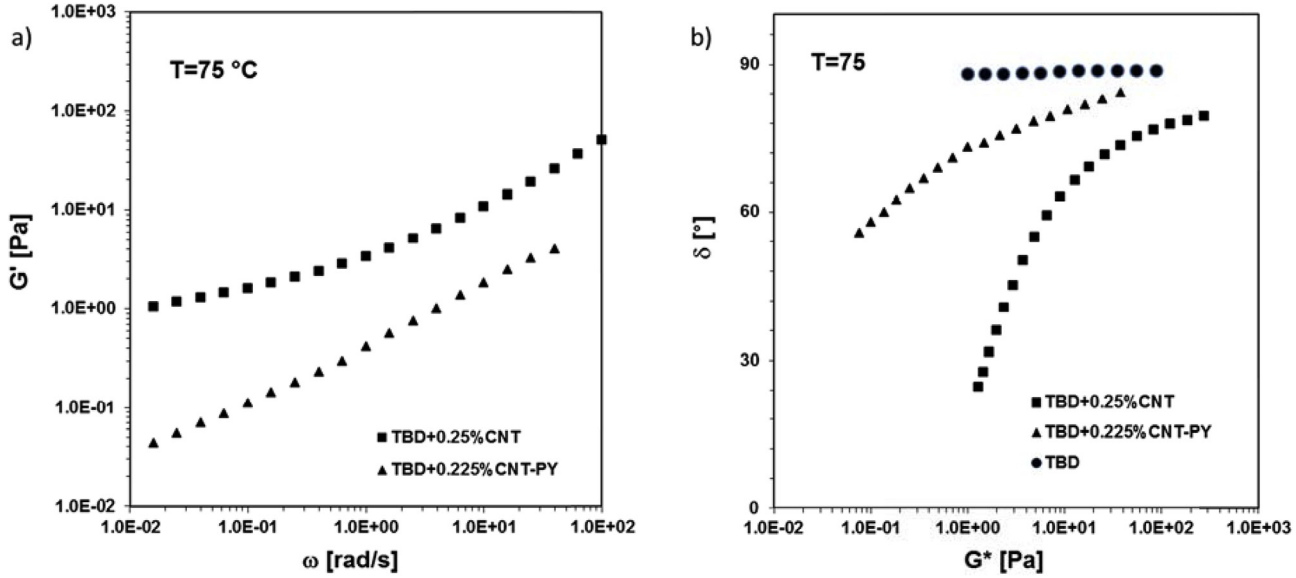

Fig. 10. Viscoelastic measurements at T = 75 °C of the TBD + 0.25%CNT, the TBD + 0.225%CNT-PY liquid dispersions and the TBD. a) Storage modulus (G′) vs frequency (ω) for the TBD + 0.25%CNT and the TBD + 0.225%CNT-PY liquid dispersions; b) Van Gurp Palmen plot.

highlights that, compared to Pyrene functionalized CNTs, the unfunctionalized CNTs tend to assume a less tortuous conformation. It looks like that unfunctionalized CNTs, less bonded to the epoxy matrix, are free to assume the most energetically favourable conformation. This relevant result could be due to the π–π stacking interactions between conjugated molecules and the graphitic sidewall of CNTs before the curing process of the nanocomposite. Compounds with the pyrene moiety could be adsorbed irreversibly onto the surface of CNTs through π–π interactions as it was already found in literature for similar compounds (N-succinimidyl-1-pyrenebutanoate) onto the surface of SWCNTs [39,40].

Furthermore, the 1-Pyrenebutyric acid, strongly bonded to the nanotube walls, is able to form strong interactions with the hosting matrix also for the presence of –COOH groups which are responsible of hydrogen bonding interactions with the –OH groups of the hosting epoxy resin. In addition, the aromatic rings of the epoxy precursor TGMDA and those of the hardener agent (DDS) in the epoxy formulation are also expected, for their chemical nature, to form attractive interactions between the hosting matrix and 1-pyrenebutyric acid of the functionalized nanofiller.

3.2.3. Electrical characterization

In such composites, the electrical properties are related to the morphology of the network formed by electrically conductive filler

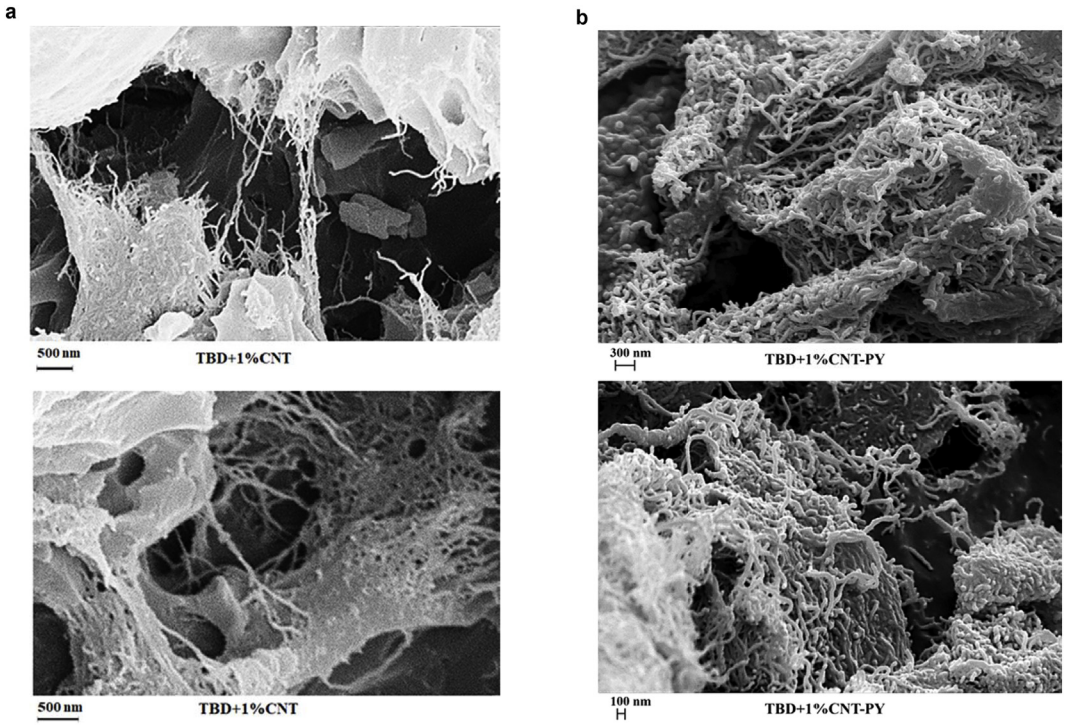

Fig. 11. a. SEM images of epoxy-based composites filled with 1.0 wt% loading of unfunctionalized CNT. **b**. SEM images of epoxy-based composites filled with 1.0 wt % loading of CNT-PY.

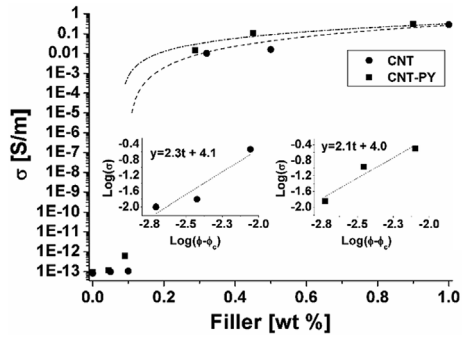

Fig. 12. DC volume conductivity of the nanocomposites versus filler weight percentage. The inset shows the log-log plot of the electrical conductivity as a function of (ϕ-ϕ_c) with a linear fit for composites reinforced with pristine CNT (on the left) and functionalized CNT-PY (on the right).

particles sufficiently close to allow, in the limit of a certain cut-off distance, the electrical conduction via tunneling effect, since an inevitable thick insulating polymer layer wraps around the outer shells of CNTs limiting the direct contact [41]. In particular, for low values of filler amount, the percolation network is not formed and the composite exhibits an electrical conductivity of the order of pS/m, typical of insulating materials. Otherwise, as soon as the filler concentration exceeds a critical value (i.e. ϕ_c, electrical percolation threshold, EPT), the conductivity increases sharply (by several orders of magnitude) following the classical power law:

$$\sigma = \sigma_0(\phi-\phi_c)^t \quad (1)$$

where σ_0 is the intrinsic conductivity of the filler and t is a critical exponent depending on the dimensionality of the percolating structure. Fig. 12 shows the DC volume conductivity (i.e. σ), measured at room temperature, as a function of the filler concentration (wt %) for the two types of MWCNTs considered in this study (unfunctionalized CNT and functionalized CNT-PY). In Fig. 12, the amount of filler (wt%) has been calculated subtracting the weight of the pyrene part bound to the nanotubes. Using this calculation methodology, the weight percentage on the x axis refer exclusively to the multi wall carbon nanotubes amount. Therefore, since in the functionalized CNT-PY, the contribution of the functional groups has been subtracted, in Fig. 12 the data are reported with a slight misalignment between the concentrations of the two fillers.

More in details, as concerns the EPT, the experimental characterization doesn't reveal remarkable difference achieved with the two fillers (i.e. pristine and functionalized MWCNTs) since for both the respective values fall in the similar restricted range, i.e. [0.1–0.32] wt% and [0.1–0.28] wt%, at least for the analyzed concentrations. Several experimental and theoretical studies have been focused on the identification of the critical factors which affect the EPT. Based on excluded volume theory [42] and numerical simulations [43,44] strong correlations were identified between EPT and aspect ratio (AR) of fillers. In particular, it has been observed that the electrical percolation threshold decreases with increasing the aspect ratio in agreement with the following expression:

$$EPT \propto \frac{1}{AR} \quad (2)$$

In light of this predicted trend, the estimated similar EPTs values for the two composites suggest similar ARs for the considered fillers, i.e. the proposed non-covalent functionalization of MWCNTs seems to preserve the carbon nanotubes structure. Moreover, Fig. 12 shows that an appreciable improvement for the electrical conductivity of the composites reinforced with functionalized CNT-PY with respect the pristine CNT case for each filler concentration above the EPT is observed. In fact, higher conductivity values are achieved with lower amount of conductive filler. As for example, if the σ of the composites reinforced with 0.5 wt% of pristine CNT and 0.45 wt% of functionalized CNT-PY are compared, values of 0.015 S/m against 0.109 S/m are reported in Fig. 12, showing an increment of an order of magnitude of the electrical property with a decrement of 10% of the conductive filler amount. It means that the proposed functionalization leads to reduce the amount of conductive filler that is required to reach a specific electrical property in the post-percolation. Finally, the characteristic parameters of the percolation law can be estimated from the curves (insets of Fig. 12), reporting the log-log plots of the experimental conductivity vs. filler concentration. In particular, the value for the critical exponent t can be obtained as the slope of the linear fit. The estimated values, i.e. 2.3 and 2.1 for pristine and functionalized MWCNTs reinforced composites respectively, are found to agree for both with universal values indicative of a three-dimensional organization of the percolating structure typically obtained with a one-dimensional filler type. It is worth noting that the same CNTs employed in this work have been covalently functionalized with -COOH groups [9] and -NH_2 groups [11]. The electrical conductivity has been evaluated for epoxy-based nanocomposites containing both unfunctionalized and functionalized carbon nanotubes. Furthermore, the authors of Ref. [11] have also studied the effect of unfunctionalized Double Wall Carbon Nanotubes (DWCNTs) and DWCNTs functionalized with -NH_2 groups on the electrical properties of the formulated nanocomposites.

For all analyzed nanocomposites, the covalent functionalization determines a decrease in the electrical properties: a) for the DWCNTs based-epoxy composites, the -NH_2 groups, covalently bonded to the wall of nanotubes, determines an increase in the EPT value and, in addition, a decrease in the electrical conductivity value beyond the EPT; b) for MWCNTs based-epoxy composites, the same functional group determines a strong increase in EPT, as expected by the constatation that, in the analyzed range of “Filler content”, no plateau is reached in the specific conductivity [11]. Very similar results were obtained with -COOH groups covalently bonded to MWCNTs [9]. Ma et al. also studied the effects of silane functionalization of multi-wall carbon nanotubes (CNTs) on properties of CNT/epoxy nanocomposites. They found that grafting silane molecules onto the CNT surface improved the dispersion of CNTs in epoxy along with much enhanced mechanical and thermal properties, but the electrical conductivity decreased due to the wrapping of CNTs with non-conductive silane molecules [10].

In conclusion, the effect of the covalent functionalization, which determines the formation of defects in the wall of CNTs due to the change in the hybridization state of part of carbon atoms (from sp^2 to sp^3) causes a deterioration in the electrical properties of the nanocomposites. The reason of a such deterioration can be due to different factors: the extent of the loss in the π electrons delocalization, and/or different morphological rearrangements of CNTs in the polymeric matrix, and/or the presence of an insulating skin around the CNTs [9]. It is most likely that within certain ranges of defect percentage (due to the functional groups attached to the wall of CNTs), the electrical properties are mainly dominated by the presence of the insulating skin around the nanotubes [9]. The non-covalent functionalization performed and discussed in this paper is able to overcome the above drawbacks as highlighted by the preservation of the electrical performance.

4. Conclusion

The functionalization of MWCNTs by π-stacking interactions between nanofiller and a pyrene derivative has been explored. A preliminary morphological and thermogravimetric characterization of both pristine and functionalized nanofiller has been carried out in order to highlight any significant differences. Functionalized and unfunctionalized MWCNTs have been dispersed in an epoxy-based matrix and the effect of the functionalization on rheological, morphological and electrical properties has been evaluated. Rheological properties

highlighted a very interesting benefit of this type of functionalization; beside preventing agglomeration during the filler dispersion, this functionalization may efficiently contribute to decrease the viscosity of the nanocomposites; contrasting a very relevant drawback typical of nanocomposites loaded with MWCNT even at a concentration beyond the electrical percolation threshold (EPT). Because no damage of MWCNTs occurs, sp^2 hybridization of carbon atoms is preserved together with the π-electron delocalization of aromatic rings. As a consequence, no decrease in the performance of the electrical properties of the formulated nanocomposites is detected. Furthermore, an improvement in the electrical properties is found with respect to typical covalent functionalizations and no increase in the EPT value and decrease in the electrical conductivity are observed with respect to the unfunctionalized MWCNTs. The benefit of methods of functionalization of CNTs based on non-covalent interaction without destroying the intrinsic sp^2-hybridized structure of the nanotube sidewall, so that the original electronic structure and properties of CNTs can be preserved, has been already reported in literature by other authors in many fields of the science and of the nanotechnologies. Nanomed et al. studied this kind of functionalization and its application in nanomedicine [45]. Chen et al. reported the noncovalent sidewall functionalization of single-walled carbon nanotubes (SWCNTs) for protein immobilization [39] noting that it is imperative to functionalize the sidewalls of SWNTs in noncovalent ways to preserve the sp^2 nanotube structure and thus their electronic characteristics [39]. The equilibrium tube-molecule distance, adsorption energy, and charge transfer have also been studied using calculation models by Zhao et al. [46]. Their results highlighted that noncovalent functionalization of carbon nanotubes by aromatic molecules is an efficient way to control the electronic properties of carbon nanotubes [46].

In this paper, this kind of functionalization has been employed to develop multifunctional structural nanocomposites evidencing also another relevant benefit, which consists in the possibility to contrast the increase in viscosity values due to the nanoparticles embedded in the formulations. This result is not trivial for many industrial applications, where the increase in the viscosity of nanofilled formulations prohibits their use and hence does not allow to exploit the advantages of the nanocomposites in real applications. As an instance, in aeronautics or automotive fields the manufacturing process of Carbon Fiber Reinforced Composites (CFRCs), such as liquid injection technologies (infusion, RTM) etc. requires the control of the viscosity. The incorporation of CNTs in the resin determines an increase of the viscosity, which in turn can negatively affect the impregnation of the CFs [14]. The possibility to hinder the increase in the viscosity due to the presence of the nanofiller without compromising the electrical conductivity of the resin impregnating the CFs constitutes a significant step forward in the process of fulfilling industrial requirements for the manufacturing of structural multifunctional composites.

Acknowledgements

The research leading to these results has received funding from the European Union Horizon 2020 Programme under Grant Agreement EU Project 760940-MASTRO.

References

[1] Dresselhaus MS, Dresselhaus G, Charlier JC, Hernandez E. Electronic, thermal and mechanical properties of carbon nanotubes. Philosophical transactions. Mathematical, physical and engineering sciences Royal Society of London; 2004. p. 2065–98. http://dx.doi.org/10.1098/rsta.2004.1430. 362(1823).

[2] El Moumena A, Tarfaouia M, Lafdi K. Mechanical characterization of carbon nanotubes based polymer composites using indentation tests. Compos B Eng 2017;114:1–7https://doi.org/10.1016/j.compositesb.2017.02.005.

[3] Jogi B, Sawant M, Kulkarni M, Brahmankar P. Dispersion and performance properties of carbon nanotubes (CNTs) based polymer composites: a review. J Encapsulation Adsorpt Sci 2012;2(4):69–78. http://dx.doi.org/10.4236/jeas.2012.24010.

[4] Bose S, Khare RA, Moldenaers P. Assessing the strengths and weaknesses of various types of pre-treatments of carbon nanotubes on the properties of polymer/carbon nanotubes composites: a critical review. Polymer 2010;51(5):975–93https://doi.org/10.1016/j.polymer.2010.01.044.

[5] Chen L, Xie H, Yu W. Prof. Jose Mauricio Marulandaeditor. Functionalization methods of carbon nanotubes and its applications, carbon nanotubes applications on electron devices InTech; 2011. http://dx.doi.org/10.5772/18547 Available from: https://www.intechopen.com/books/carbon-nanotubes-applications-on-electron-devices/functionalization-methods-of-carbon-nanotubes-and-its-applications.

[6] Sun YP, Fu K, Lin Y, Huang W. Functionalized carbon nanotubes: properties and applications. Acc Chem Res 2002;35(12):1096–104. http://dx.doi.org/10.1021/ar010160v.

[7] Ma PC, Siddiqui NA, Marom G, Kim JK. Dispersion and functionalization of carbon nanotubes for polymer-based nanocomposites: a review. Compos Part A Appl Sci Manuf 2010;41(10):1345–67https://doi.org/10.1016/j.compositesa.2010.07.003.

[8] Kuzmany H, Kukovecz A, Simon F, Holzweber M, Kramberger C, Pichler T. Functionalization of carbon nanotubes. Synth Met 2004;141(1–2):113–22https://doi.org/10.1016/j.synthmet.2003.08.018.

[9] Guadagno L, De Vivo B, Di Bartolomeo A, Lamberti P, Sorrentino A, Tucci V, et al. Effect of functionalization on the thermo-mechanical and electrical behavior of multi-wall carbon nanotube/epoxy composites. Carbon 2011;49(6):1919–30https://doi.org/10.1016/j.carbon.2011.01.017.

[10] Ma PC, Kim JK, Tang BZ. Effects of silane functionalization on the properties of carbon nanotube/epoxy nanocomposites. Compos Sci Technol 2007;67(14):2965–72. 2007 https://doi.org/10.1016/j.compscitech.2007.05.006.

[11] Gojny FH, Wichmann MHG, Fiedler B, Kinloch IA, Bauhofer W, Windle AH, et al. Evaluation and identification of electrical and thermal conduction mechanisms in carbon nanotube/epoxy composites. Polymer 2006;47(6):2036–45https://doi.org/10.1016/j.polymer.2006.01.029.

[12] Song SH, Park KH, Kim BH, Choi YW, Jun GH, Lee DJ, et al. Enhanced thermal conductivity of epoxy–graphene composites by using non-oxidized graphene flakes with non-covalent functionalization. Adv Mater 2013;25(5):732–7. http://dx.doi.org/10.1002/adma.201202736.

[13] Georgakilas V, Tiwari JN, Kemp KC, Perman JA, Bourlinos AB, Kim KS, et al. Noncovalent functionalization of graphene and graphene oxide for energy materials, biosensing, catalytic, and biomedical applications. Chem Rev 2016;116(9):5464–519. http://dx.doi.org/10.1021/acs.chemrev.5b00620.

[14] Guadagno L, Raimondo M, Vietri U, Vertuccio L, Barra G, De Vivo B, et al. Effective formulation and processing of nanofilled carbon fiber reinforced composites. RSC Adv 2015;5(8):6033–42https://doi.org/10.1039/C4RA12156B.

[15] Guadagno L, Raimondo M, Vittoria V, Vertuccio L, Naddeo C, Russo S, et al. Development of epoxy mixtures for application in aeronautics and aerospace. RSC Adv 2014;4(30):15474–88https://doi.org/10.1039/C3RA48031C.

[16] Nobile MR, Raimondo M, Lafdi K, Fierro A, Rosolia S, Guadagno L. Relationships between nanofiller morphology and viscoelastic properties in CNF/epoxy resins. Polym Compos 2015;36(6):1152–60. http://dx.doi.org/10.1002/pc.23362.

[17] Guadagno L, Raimondo M, Vertuccio L, Mauro M, Guerra G, Lafdi K, et al. Optimization of graphene-based materials outperforming host epoxy matrices. RSC Adv 2015;5(46):36969–78https://doi.org/10.1039/C5RA04558D.

[18] Guadagno L, Vietri U, Raimondo M, Vertuccio L, Barra G, De Vivo B, et al. Correlation between electrical conductivity and manufacturing processes of nanofilled carbon fiber reinforced composites. Compos B Eng 2015;80:7–14https://doi.org/10.1016/j.compositesb.2015.05.025.

[19] Vertuccio L, Guadagno L, Spinelli G, Russo S, Iannuzzo G. Effect of carbon nanotube and functionalized liquid rubber on mechanical and electrical properties of epoxy adhesives for aircraft structures. Compos B Eng 2017;129:1–10. http://dx.doi.org/10.1016/j.compositesb.2017.07.021.

[20] Guadagno L, Naddeo C, Raimondo M, Barra G, Vertuccio L, Sorrentino A, et al. Development of self-healing multifunctional materials. Compos B Eng 2017;128:30–8https://doi.org/10.1016/j.compositesb.2017.07.003.

[21] Raimondo M, Guadagno L, Speranza V, Bonnaud L, Dubois P, Lafdi K. Multifunctional graphene/POSS epoxy resin tailored for aircraft lightning strike protection. Compos B Eng 2018;140:44–56https://doi.org/10.1016/j.compositesb.2017.12.015.

[22] Zhang Y, Yuan S, Zhou W, Xu J, Li Y. Spectroscopic evidence and molecular simulation investigation of the pi-pi interaction between pyrene molecules and carbon nanotubes. J Nanosci Nanotechnol 2007;7(7):2366–75https://doi.org/10.1166/jnn.2007.412.

[23] Pötschke P, Fornes TD, Paul DR. Rheological behavior of multiwalled carbon nanotube/polycarbonate composites. Polymer 2002;43(11):3247–55https://doi.org/10.1016/S0032-3861(02)00151-9.

[24] Du F, Scogna RC, Zhou W, Brand S, Fischer JE, Winey KI. Nanotube networks in polymer nanocomposites: rheology and electrical conductivity. Macromolecules 2004;37(24):9048–55. http://dx.doi.org/10.1021/ma049164g.

[25] Pötschke P, Abdel-Goad M, Alig I, Dudkin S, Lellinger D. Rheological and dielectrical characterization of melt mixed polycarbonate-multiwalled carbon nanotube composites. Polymer 2004;45(26):8863–70https://doi.org/10.1016/j.polymer.2004.10.040.

[26] Song YS. Rheological characterization of carbon nanotubes/poly(ethylene oxide) composites. Rheol Acta 2006;46(2):231–8https://doi.org/10.1007/s00397-006-0137-8.

[27] Abbasi S, Carreau PJ, Derdouri A, Moan M. Rheological properties and percolation in suspensions of multiwalled carbon nanotubes in polycarbonate. Rheol Acta 2009;48:943–59https://doi.org/10.1007/s00397-009-0375-7.

[28] Hobbie EK. Shear rheology of carbon nanotube suspensions. Rheol Acta

2010;49(4):323–34https://doi.org/10.1007/s00397-009-0422-4.
[29] Nobile MR. Rheology of polymer-carbon nanotube composite melts. In: McNally T, Pötschke P, editors. Polymer-carbon nanotube composites. Preparation, properties and application. Cambridge: Woodhead Publishing; 2011. p. 428–81https://doi.org/10.1533/9780857091390.2.428.
[30] Yearsley KM, Mackley MR, Chinesta F, Leygue A. The rheology of multiwalled carbon nanotube and carbon black suspensions. J Rheol 2012;56(6):1465–90https://doi.org/10.1122/1.4751871.
[31] Urena-Benavides EE, Kayatin MJ, Davis VA. Dispersion and rheology of multiwalled carbon nanotubes in unsaturated polyester resin. Macromolecules 2013;46(4):1642–50. http://dx.doi.org/10.1021/ma3017844.
[32] Di Maio L, Garofalo E, Scarfato P, Incarnato L. Effect of polymer/organoclay composition on morphology and rheological properties of polylactide nanocomposites. Polym Compos 2015;36(6):1135–44. http://dx.doi.org/10.1002/pc.23424.
[33] Nobile MR, Valentino O, Morcom M, Simon GP, Landi G, Neitzert HC. The Effect of the nanotube oxidation on the rheological and electrical properties of CNT/HDPE nanocomposites. Polym Eng Sci 2017;57(7):665–73. http://dx.doi.org/10.1002/pen.24572.
[34] Van Gurp M, Palmen J. Time-temperature superposition for polymeric blends. Rheol Bull 1998;67:5–8.
[35] Wu D, Wu L, Zhang M. Rheology of multi-walled carbon nanotube/poly(butylene terephthalate) composites. J Polym Sci B Polym Phys 2007;45(16):2239–51. http://dx.doi.org/10.1002/polb.21233.
[36] Amr IT, Al-Amer A, Thomas SP, Al-Harthi M, Girei SA, Sougrat R, et al. Effect of acid treated carbon nanotubes on mechanical, rheological and thermal properties of polystyrene nanocomposites. Compos B Eng 2011;42(6):1554–61https://doi.org/10.1016/j.compositesb.2011.04.013.
[37] Wang M, Wang W, Liu T, Zhang WD. Melt rheological properties of nylon 6/multi-walled carbon nanotube composites. Compos Sci Technol 2008;68(12):2498–502https://doi.org/10.1016/j.compscitech.2008.05.002.
[38] Šupová M, Martynková GS, Barabaszová K. Effect of nanofillers dispersion in polymer matrices: a review. Sci Adv Mater 2011;3(1):1–25. http://dx.doi.org/10.1166/sam.2011.1136.
[39] Chen RJ, Zhang Y, Wang D, Dai H. Noncovalent sidewall functionalization of single-walled carbon nanotubes for protein immobilization. J Am Chem Soc 2001;123(16):3838–9. http://dx.doi.org/10.1021/ja010172b.
[40] Zare K, Gupta VK, Moradi O, Makhlouf ASH, Sillanpää M, Nadagouda MN, et al. A comparative study on the basis of adsorption capacity between CNTs and activated carbon as adsorbents for removal of noxious synthetic dyes: a review. J Nanostruc Chem 2015;5(2):227–36https://doi.org/10.1007/s40097-015-0158-x.
[41] De Vivo B, Lamberti P, Spinelli G, Tucci V. A morphological and structural approach to evaluate the electromagnetic performances of composites based on random networks of carbon nanotubes. J Appl Phys 2014;115(15):154311https://doi.org/10.1063/1.4871670.
[42] Balberg I, Binenbaum N, Wagner N. Percolation thresholds in the three-dimensional sticks system. Phys Rev Lett 1984;52(17):1465–8https://doi.org/10.1103/PhysRevLett.52.1465.
[43] Eken AE, Tozzi EJ, Klingenberg DJ, Bauhofer W. A simulation study on the combined effects of nanotube shape and shear flow on the electrical percolation thresholds of carbon nanotube/polymer composites. J Appl Phys 2011;109(8):084342https://doi.org/10.1063/1.3573668.
[44] De Vivo B, Lamberti P, Spinelli G, Tucci V. Numerical investigation on the influence factors of the electrical properties of carbon nano tubes-filled composites. J Appl Phys 2013;113(24):244301https://doi.org/10.1063/1.4811523.
[45] Sadegh H, Shahryari-ghoshekandi R. Functionalization of carbon nanotubes and its application in nanomedicine: a review. Nanomed J 2015;2(4):231–48. http://dx.doi.org/10.7508/nmj. 2015.04.001.
[46] Zhao J, Lu JP. Noncovalent functionalization of carbon nanotubes by aromatic organic molecules. Appl Phys Lett 2003;82(21):3746–8https://doi.org/10.1063/1.1577381.